International Journal of Biological Macromolecules 242 (2023) 124742

Contents lists available at ScienceDirect

International Journal of Biological Macromolecules

journal homepage: www.elsevier.com/locate/ijbiomac

Thermoplastic starch/bentonite clay nanocomposite reinforced with vitamin B_2: Physicochemical characteristics and release behavior

Abolfazl Heydari [a,b,*], Milad KhajeHassani [c], Haniyeh Daneshafruz [c], Sepideh Hamedi [d,**], Faeze Dorchei [a], Mário Kotlár [e], Fahimeh Kazeminava [f], Samahe Sadjadi [g], Farideh Doostan [h,**], Ivan Chodak [a], Hassan Sheibani [c]

[a] Polymer Institute of the Slovak Academy of Sciences, Dúbravská cesta 9, 845 41 Bratislava, Slovakia
[b] National Institute of Rheumatic Diseases, Nábrežie I. Krasku 4782/4, 921 12 Piešťany, Slovakia
[c] Department of Chemistry, Shahid Bahonar University of Kerman, Kerman 76169, Iran
[d] Faculty of New Technologies Engineering, Shahid Beheshti University, Tehran, Iran
[e] Centre for Nanodiagnostics of Materials, Faculty of Materials Science and Technology, Slovak University of Technology, Vazovova 5, Bratislava 812 43, Slovakia
[f] Stem Cell Research Center, Tabriz University of Medical Sciences, Tabriz, Iran
[g] Gas Conversion Department, Faculty of Petrochemicals, Iran polymer and Petrochemical Institute, PO Box 14975-112, Tehran, Iran
[h] Endocrinology and Metabolism Research Center, Institute of Basic and Clinical Physiology Sciences, Kerman University of Medical Sciences, Kerman, Iran

ARTICLE INFO

Keywords:
Thermoplastic starch
Vitamin B_2
Active packaging

ABSTRACT

This study presents the development and characterization of a nanocomposite material, consisting of thermoplastic starch (TPS) reinforced with bentonite clay (BC) and encapsulated with vitamin B_2 (VB). The research is motivated by the potential of TPS as a renewable and biodegradable substitute for petroleum-based materials in the biopolymer industry. The effects of VB on the physicochemical properties of TPS/BC films, including mechanical and thermal properties, water uptake, and weight loss in water, were investigated. In addition, the surface morphology and chemical composition of the TPS samples were analyzed using high-resolution SEM microscopy and EDS, providing insight into the structure-property relationship of the nanocomposites. The results showed that the addition of VB significantly increased the tensile strength and Young's modulus of TPS/BC films, with the highest values observed for nanocomposites containing 5 php of VB and 3 php of BC. Furthermore, the release of VB was controlled by the BC content, with higher BC content leading to lower VB release. These findings demonstrate the potential of TPS/BC/VB nanocomposites as environmentally friendly materials with improved mechanical properties and controlled release of VB, which can have significant applications in the biopolymer industry.

1. Introduction

Starch, as one of the most promising candidates in the biopolymer industry, has been widely considered, since it is completely biodegradable, available from renewable resources, abundant in nature, and cost-effective. However, high brittleness is one of the disadvantages, which is seen in native starch as a plastic material. Therefore, by adding a suitable plasticizer, it can be converted to thermoplastic starch (TPS) under special thermal and shear conditions [1–3]. This plastification process leads to the destruction of crystallinity and increase in chain flexibility [4]. However, the main shortcoming of TPS is the recrystallization phenomena caused by its hydrophilic character, as it leads to unsatisfactory mechanical properties during storage [1]. The incorporation of filler in the polymer matrix can be considered as one of the most practical strategies to improve the mechanical properties of starch-based films, as well as one of the important approaches to develop barrier properties to prevent the penetration of moisture and oxygen [5–7]. Layered silicates have proven to be effective reinforcing agents to improve barrier and mechanical properties of the polymer matrix. The incorporation of inorganic silicate layers provides a barrier against oxygen and water molecules, and also increases the strength and modulus strength of the resulting nanocomposites [8]. A variety of layered

* Correspondence to: A. Heydari, Polymer Institute of the Slovak Academy of Sciences, Dúbravská cesta 9, 84541 Bratislava, Slovakia.
** Corresponding authors.
E-mail addresses: abolfazl.heydari@savba.sk (A. Heydari), se_hamedi@sbu.ac.ir (S. Hamedi), f_doostan@kmu.ac.ir (F. Doostan).

https://doi.org/10.1016/j.ijbiomac.2023.124742
Received 12 February 2023; Received in revised form 3 April 2023; Accepted 1 May 2023
Available online 5 May 2023

Table 1
Sample codes and composition of the TPS composites filled with bentonite clay (BC) and vitamin B_2 (VB). The numbers after BC and VB in the sample codes represent the amount of BC and VB in php, respectively.

Sample code	Starch (g)	Glycerol (g)	BC (g)	VB (g)
TPS	100	50	0	0
TPS/BC3	100	50	3	0
TPS/BC10	100	50	10	0
TPS/VB1	100	50	0	1
TPS/VB5	100	50	0	5
TPS/VB10	100	50	0	10
TPS/BC3/VB1	100	50	3	1
TPS/BC3/VB5	100	50	3	5
TPS/BC3/VB10	100	50	3	10
TPS/BC10/VB1	100	50	10	1
TPS/BC10/VB5	100	50	10	5
TPS/BC10/VB10	100	50	10	10

silicates, including montmorillonite, bentonite, hectorite, saponite, and other modified cationic compounds, have been explored for their potential as reinforcing agents. Among these, bentonite clay is particularly attractive due to its low cost, large availability, and environmentally benign nature [9–12]. On the other hand, nanocomposite films incorporating bioactive molecules, such as antimicrobials, antioxidants, and vitamins increasingly popular in the cosmetic, pharmaceutical, nutraceutical, and food industries [13]. Vitamins, which are classified into fat-soluble (vitamin A, D, E, K, and B_2) and water-soluble (vitamin C, B_6, B_{12}, and folate) categories, are among the most commonly used bioactive molecules in nanocomposites. [14].

Vitamin B_2, also known as riboflavin, is one of the essential water-soluble vitamins for humans [15]. Vitamin B_2 plays an important role in the metabolism of carbohydrates, lipids, and proteins and is crucial for the generation of biological energy in the electron-transport system. Vitamin B_2 is an abundant, naturally occurring chemical existing in various food like milk, dairy products, fish, meats, fruit, and vegetables [16]. This vitamin is also essential for living organisms and plays a vital role in the production and regulation of certain hormones, and the formation of red blood cells [17]. Vitamin B_2 is known as a photosensitizer, which can produce reactive oxygen species (ROS) at a certain wavelength leading to the deactivation of malignant cells and pathogenic microorganisms [18,19]. Sufficient dietary or supplemental intake of vitamin B_2 has been reported to provide anti-oxidant, anti-aging, anti-inflammatory, and anti-cancer properties [20]. However, vitamin B_2 deficiency can lead to a range of symptoms, including hair loss, skin crack, depression, blurred vision, swollen mouth, and tongue [21]. Since the human body is unable to synthesize vitamin B_2, it must be obtained through dietary sources [22]. Nevertheless, vitamins are vulnerable to light, heat, and oxidation, which can degrade their bioactivity. The encapsulation of vitamin B_2 in a polymer matrix has been identified as a promising approach to protect the vitamin from environmental factors that may degrade its quality and stability [14,23–25]. Various types of polymeric materials have been investigated for this purpose, such as hyaluronic acid hydrogels [26], alginate hydrogel coated with chitosan [27], chitosan-based printed materials [28], epichlorohydrin-crosslinked β-cyclodextrin nanofibers [24], epichlorohydrin/guanidine-crosslinked β-cyclodextrin [25], ethyl cellulose-coated barium alginate beads [29], starch/polyacrylic acid [30], silk fabric [31], alginate multilayered gel microspheres [29,32], gum arabic, maltodextrin, sodium alginate, and pectin microparticles [33]. These delivery systems have shown the ability to provide controlled release of encapsulated vitamin B_2. Overall, the use of polymer-based encapsulation strategies holds great potential for enhancing the stability and efficacy of vitamin B_2 in various applications.

The development of active packaging systems using biodegradable materials is of great interest to preserve and enhance the functionality of encapsulated compounds, such as vitamin B_2 (VB). One potential material for this purpose is a biodegradable TPS/bentonite clay nanocomposite film. However, to the best of our knowledge, no previous research has explored the simultaneous incorporation of VB and bentonite clay in starch-based films. Therefore, the primary objective of this study is to evaluate the physicochemical properties of the nanocomposites based on TPS loaded with various contents of bentonite clay and VB, using the solvent casting method. The high resolution SEM microscope and EDS were used to analyze the surface morphology and chemical composition of the TPS samples. Additionally, the effects of bentonite clay and VB on the mechanical and thermal properties of TPS films, as well as their stability in water and release behavior, will be investigated.

2. Experimental

2.1. Materials

Native corn starch Meritena® 100 was supplied by Brenntag (Bratislava, Slovakia). The water content determined by drying in an oven at 100 °C for 5 h was around 12 wt%. Bentonite clay (BC) was purchased from Southern Clay Brick Co. (Texas, USA). Glycerol and vitamin B_2 (VB) were purchased from Merck (Darmstadt, Germany). Double distilled water was used in all experiments.

2.2. Preparation of TPS-bentonite clay nanocomposites reinforced with vitamin B_2

First, bentonite clay (BC) at 3 and 10 parts based on the dry weight of starch (php) were dispersed in water by sonication at ambient temperature for 10 min. Then, each suspension was added separately to a mixture containing starch, glycerol and water according to the receipt summarized in Table 1. In the next step, to prepare vitamin B_2-reinforced samples, 1, 5, and 10 php of vitamin (based on dry weight of starch) were added to starch and starch-BC solutions. The following procedure was performed to further process the mixtures. Gelatinized starch was obtained by heating a mixture of starch, BC, glycerol, VB, and water at 70 °C for 15 min while stirring continuously. Homogenization of all mixtures was achieved through sonication for 30 min, and then cast into circular molds before being dried at 45 °C in an oven for 24 h. To investigate the effects of VB and BC on the properties of TPS films, two sets of composite films were prepared - one with BC and VB and the other without BC and with VB. The composition and sample codes for each formulation are summarized in Table 1.

2.3. Physico-chemical characterization

2.3.1. Elemental analysis

Elemental analysis was performed to measure carbon, nitrogen and hydrogen contents using a Thermo scientific Flash 2000 CHN Elemental Analyzer.

2.3.2. Scanning electron microscopy (SEM) and energy dispersive X-ray spectroscopy (EDS)

Surface morphology of the TPS samples was characterized by high resolution SEM microscope Thermo Fisher Scios 2 LoVac. Images were recorded using secondary electrons (SE) at 10 kV accelerating voltage and 7 mm working distance. The chemical composition of the samples was analyzed by EDS using Thermo Scientific UltraDry EDS spectrometer with active area of 60 mm^2 at 10 kV electron accelerating voltage.

2.3.3. Mechanical properties

The mechanical properties of the prepared films were determined using an Instron 3365 universal testing machine (Instron, Massachusetts, USA). Prior to testing, dog-bone shaped specimens were manually punched using toggle press equipment with a dimension of 3.5 × 30 mm for the area of deformation during the test. The thickness of the specimens, measured using a digital caliper, was approximately 1 mm. Tests

Table 2
CHN elemental analysis results of the TPS samples containing bentonite clay (BC) and vitamin B_2 (VB).

Sample	C	N	H
TPS	39.41 ± 0.20	0	7.0 ± 0.2
TPS/BC10	37.33 ± 0.13	0	6.7 ± 0.1
TPS/VB10	40.69 ± 0.17	1.10 ± 0.03	6.81 ± 0.04
TPS/BC10/VB10	38.15 ± 0.21	0.99 ± 0.1	6.69 ± 0.15

were carried out at a speed of 1 mm·min^{-1} with deformation up to 1 % and at a speed of 50 mm·min^{-1} at higher deformations, according to ASTM D638. The mean values and standard deviations were calculated of 7 specimens for all parameters.

2.3.4. *Dynamic mechanical thermal analysis (DMTA)*

Dynamic mechanical thermal analysis (DMTA) was conducted using DMA Q800 (TA Instruments, Germany). Tests were performed in tensile mode at a frequency of 10 Hz and an amplitude of 20 μm. These measurements were performed to determine the storage modulus (G′), loss

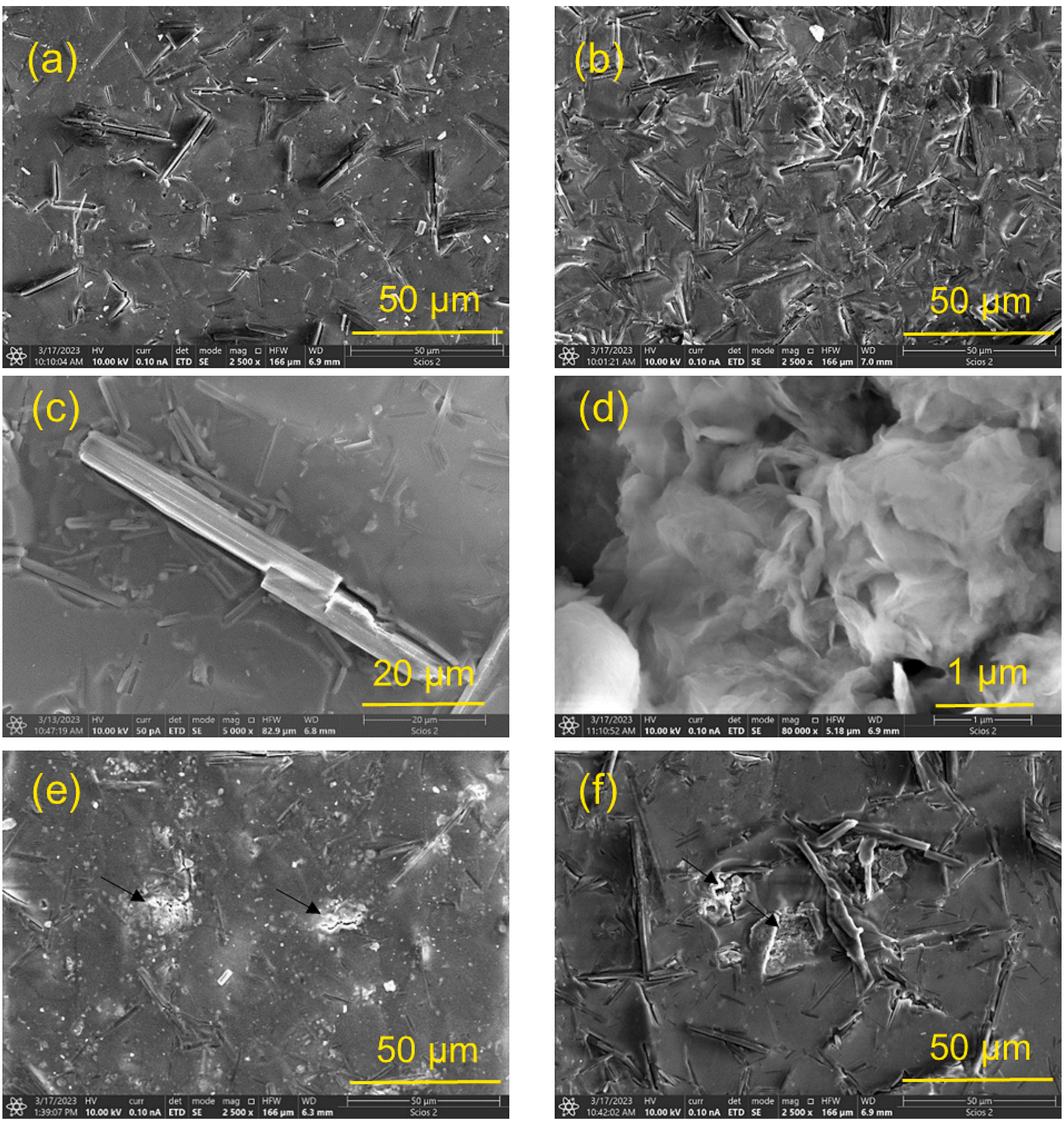

Fig. 1. SEM Images showing surface morphology of the samples with (a) 1 php (TPS/VB1) and (b) 10 php (TPS/VB10) of vitamin B_2. Higher magnification images of the (c) rod shaped vitamin B_2 particle and (d) agglomerated bentonite clay particle (image artefacts are due to charging). SEM Images showing the surface morphology of the samples with (e) 1 php (TPS/BC10/VB1) and (f) 10 php (TPS/BC10/VB10) of vitamin B_2, both with 10 php of bentonite clay (bentonite clay particles are marked with arrows).

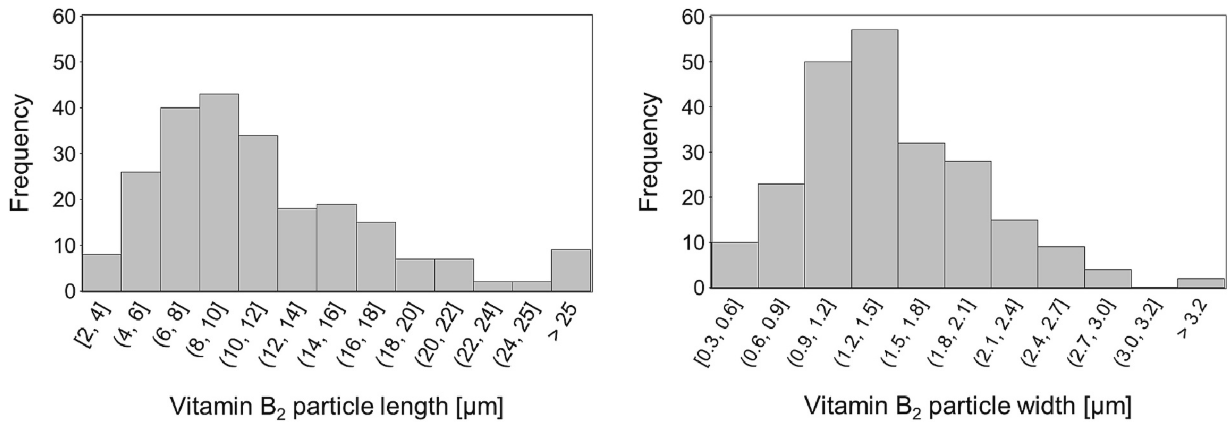

Fig. 2. Vitamin B_2 particle size distribution histograms analyzed from SEM images.

modulus (G″), and tangent of the loss angle (tan δ) of TPS composite samples (ca. 10 × 7 × 1 mm^3). The temperature range was fixed from −20 to 120 °C with a heating rate of 2 °C·min^{-1}.

2.3.5. Thermogravimetric analysis (TGA)

Thermal stability and degradation profile of the prepared TPS samples were studied using, NETZSCH STA 449F3, TGA-50 from 20 to 800 °C at 10 K·min^{-1} rate under a nitrogen atmosphere.

2.3.6. Water uptake

The water uptake ratio of the prepared samples was determined using the gravimetric method at ambient temperature. Circular discs with a diameter of 2 cm were cut from the samples and dried at 105 °C in an oven until a constant weight (W_d) was achieved. Subsequently, the dried samples were immersed in distilled water for 24 h to attain equilibrium. After removing excess water from the surface of the films, the wet weight of the swollen samples was measured (W_s). The Water uptake ratio (WU) was calculated using the Eq. (1).

$$WU\ (\%) = \frac{W_s - W_d}{W_d} \times 100 \tag{1}$$

where W_s and W_d are the weight of the swollen and dried samples, respectively.

2.3.7. Weight loss in water

For each sample, specimens with dimensions of 2 × 2 cm (W_1) were measured, and then dried at 105 °C for 5 h before being reweighed (W_2). Subsequently, triplicate specimens of each TPS sample were immersed in deionized water and kept at ambient conditions for 24 h. After filtering, the insoluble portion was dried in an oven at 60 °C for 24 h and weighed (W_3). The moisture content (MC) and percentage of the weight loss in water (W_L) were calculated according to Eqs. (2) and (3), respectively.

$$MC\ (\%) = \frac{W_1 - W_2}{W_2} \times 100 \tag{2}$$

$$W_L\ (\%) = \left(\frac{W_2 - W_3}{W_2}\right) \times 100 \tag{3}$$

2.3.8. Zeta potential of the TPS films

The Zeta potential of the TPS films containing vitamin B_2 was measured using SurPASS 3 (Anton Paar GmbH, Austria), which was equipped with an Adjustable Gap measuring cell having a measuring surface of 20 mm × 10 mm. Electrolyte solution of 1 mmol·L^{-1} KCl used for analysis at a pH of approximately 5.8. The gap height was set to approximately 100 μm by tightening the adjustment knob. The mean zeta potential (mV) is reported with the standard deviation (SD) calculated from three independent measurements ($n = 3$). These experimental conditions were adopted in accordance with standard protocols for zeta potential measurements.

2.3.9. In vitro release of vitamin B_2

The in vitro release of vitamin B2 from the prepared films was investigated in a phosphate buffer solution (PBS) with a pH of 7.4. In brief, 200 mg of TPS loaded with vitamin B2, with and without varying amounts of BC, were suspended in vials containing 20 mL of PBS. At regular time intervals, 3 mL of the solution was collected, and its absorbance was measured at 446 nm using a UV–Vis spectrophotometer (Cary 50 UV–Vis spectrophotometer, Varian, Australia). The fresh solvent with the same volume was immediately injected into the harvested vials. The cumulative release of the vitamins from the prepared films was calculated by Eq. (4).

$$\text{cumulative release}\ (\%) = \frac{M_t}{M_0} \times 100 \tag{4}$$

where M_t is the amount of released VB from the TPS at time t and M_0 is the amount of VB in the TPS samples. The experiments were performed in triplicate, and the results were recorded as an average with an error bar that represents the relative standard deviation.

3. Results and discussion

In short, in this study, thermoplastic films were synthesized based on starch biopolymer. Bentonite clay was added as reinforcement to improve the physic-chemical characteristics of the TPS. This casted film was fortified by VB. Surface morphology and chemical composition of the TPS samples was analyzed by high resolution SEM microscope and EDS. The individual and simultaneous effects of BC and VB were studied on the tensile strength of nanocomposites. Thermal stability and degradation profiles of the prepared nanocomposites were studied by TGA. The water uptake and weight loss of the synthesized nanocomposites were investigated after individual/or simultaneous incorporation of BC and VB. Finally, the release profile of VB was evaluated from the nanocomposite containing various amounts of BC.

3.1. CHN elemental analysis

CHN analysis was performed to confirm the presence of VB in TPS/BC nanocomposites. Carbon, hydrogen, and nitrogen contents of the TPS, TPS/BC, TPS/VB, and TPS/BC/VB were measured by CHN elemental analysis, and the results are summarized in Table 2. The results show the presence of nitrogen atoms in the TPS/VB10 and TPS/BC10/VB10 samples, while the nitrogen in TPS and TPS/BC10 are equal to zero. These findings suggest the presence of VB in the VB-reinforced

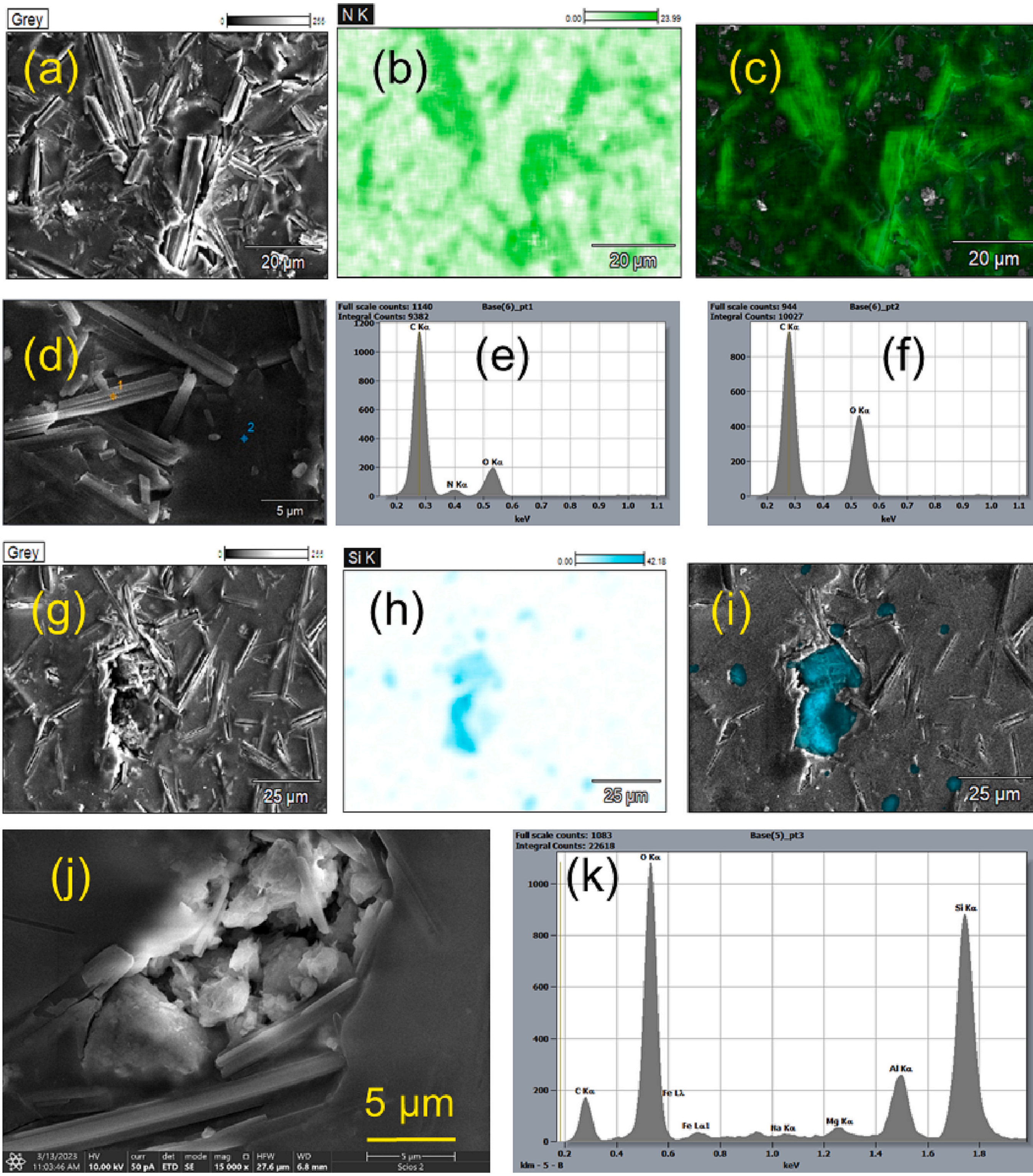

Fig. 3. (a, b, and c) EDS elemental mapping for Nitrogen of the sample TPS/VB10. EDS point spectrum from (e) VB particle and (f) starch (VB contains nitrogen in contrast to starch). (g, h, and i) EDS elemental mapping of the sample TPS/BC10/VB10 shows presence of Silicon in the BC particles. (j) SEM image of measured particle and (k) EDS point spectrum from BC particle.

samples, confirming the successful encapsulation of VB in the TPS/BC nanocomposites.

3.2. Scanning electron microscopy (SEM) and energy dispersive X-ray spectroscopy (EDS)

In this study, we investigated the properties of TPS films that were modified with vitamin B_2 (VB) and bentonite clay (BC). The presence of crystalline rod particles embedded in the starch matrix was observed in

Table 3
Mechanical properties, including tensile strength, elongation at break, and Young's modulus of the TPS nanocomposites. The concentration is shown in php as the number after each code.

Sample code	Tensile strength (MPa)	Elongation at break (%)	Young's modulus (MPa)
TPS	5.4 ± 0.7	73.8 ± 11.9	51.2 ± 23.7
TPS/BC3	5.5 ± 0.2	72.7 ± 4.6	47.7 ± 2.8
TPS/BC10	6.3 ± 0.7	49.7 ± 7.0	138.7 ± 60.4
TPS/VB1	4.9 ± 0.4	89.5 ± 13.8	50.0 ± 13.9
TPS/VB5	3.8 ± 1.0	57.5 ± 11.8	37.3 ± 8.4
TPS/VB10	3.4 ± 0.7	41.4 ± 7.4	28.4 ± 1.8
TPS/BC3/VB1	5.7 ± 0.3	81.1 ± 5.8	54.1 ± 5.2
TPS/BC3/VB5	7.6 ± 1.4	62.4 ± 12.1	205.6 ± 46.1
TPS/BC3/VB10	5.4 ± 0.5	71.1 ± 2.5	88.5 ± 26.1
TPS/BC10/VB1	6.6 ± 1.4	43.7 ± 9.1	159.9 ± 72.6
TPS/BC10/VB5	8.0 ± 2.3	39.3 ± 8.6	246.2 ± 73.4
TPS/BC10/VB10	7.0 ± 0.2	47.9 ± 3.5	169.6 ± 22.7

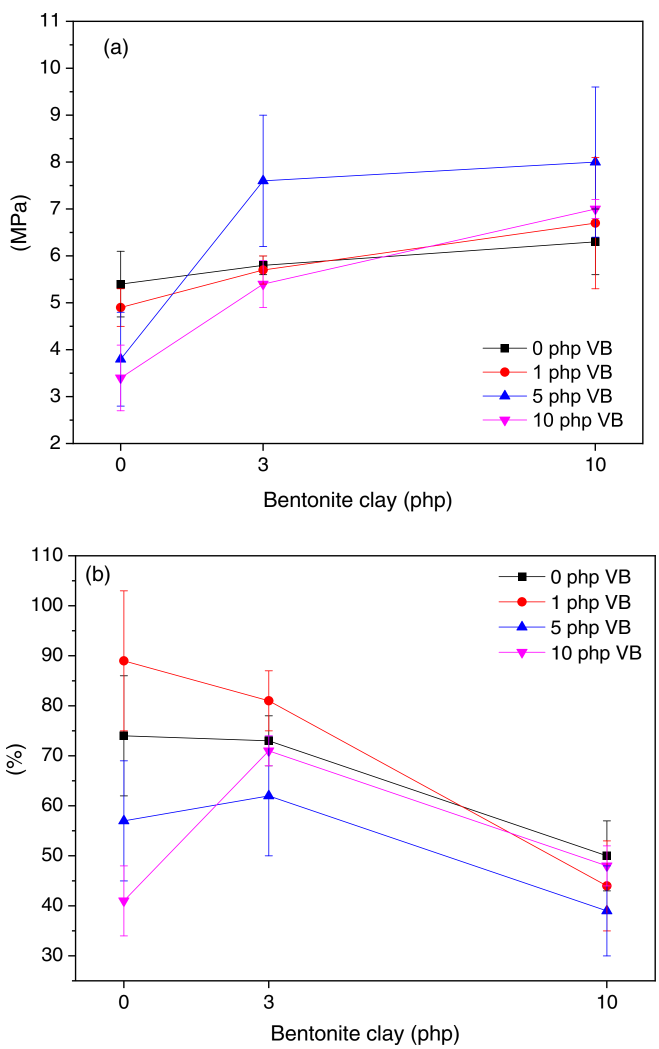

Fig. 4. Dependence of bentonite clay (BC) and vitamin B_2 (VB) contents on (a) ultimate tensile strength and (b) strain at break of the TPS nanocomposite films.

samples that contained VB (TPS/VB1 - TPS/VB10) (Fig. 1a, b, and c). The density of these rod particles varied depending on the amount of VB. Furthermore, TPS/BC nanocomposites reinforced with VB (TPS/BC10/VB1- TPS/BC10/VB10) were found to contain rod-shaped VB particles and BC agglomerates (Fig. 1d, e, and f). These observations suggest that the addition of VB and BC can enhance the structural properties of TPS films. The varying densities of the rod particles in TPS films containing VB attributed to the amount of VB present during sample preparation. Overall, our results demonstrate the potential of incorporating VB and BC into TPS films for improved performance in various applications.

The evaluation of SEM images for samples with VB content (TPS/VB1 - TPS/VB10) yielded a log-normal VB particle size distribution, as depicted in Fig. 2. However, it is worth considering that the observed distribution curves may have been influenced by the possible breaking of longer particles during the sample preparation process. The peak lengths and widths of the particles were found to be 9 and 1.2 μm, respectively. The bentonite particles appeared (Fig. 1d) as porous agglomerates with a platelet structure, with sizes ranging from hundreds of nanometers up to micrometers. The size of the platelets within an agglomerate was observed to be in the range of tens of nanometers.

EDS analysis was performed to discriminate between VB and starch grains, and to determine the elemental composition of BC. The analysis results, as presented in Fig. 3a–f, demonstrate the presence of nitrogen in VB crystalline rod particles in the samples, which allows for their discrimination from starch grains. On the other hand, the EDS analysis of BC, as shown in Fig. 3g–k, revealed the presence of Si, Al, Mg, O, Fe, and Na, which is consistent with the characteristic composition of BC. The observed elemental composition confirms the presence of BC and its constituents in the samples.

3.3. Mechanical properties

The effect of bentonite clay (BC) and vitamin B2 (VB) on the mechanical properties of thermoplastic starch (TPS) nanocomposite films was investigated. The values of mechanical properties, including tensile stress, elongation at the break, and Young's modulus are summarized in Table 3. Moreover, Fig. 4 represents the dependence of BC and VB contents on the ultimate tensile strength and strain at break of the TPS nanocomposite films. The results showed that the addition of BC slightly increased the ultimate tensile strength and Young's modulus of the TPS nanocomposite film while reducing its strain at break. The strong interaction between starch and BC limited the plasticization effect of glycerol, resulting in the anti-plasticization effect of BC, which were consistent with the previous published data [34–37]. This was attributed to the optimized number of reinforcing elements available to carry the applied load and deflecting cracks due to the dispersion of clay nanolayers in the TPS matrix [9,38].

The corresponding results of mechanical properties for the TPS films containing vitamin B_2 can be seen in Fig. 4 and Table 3. These results exhibit a decrease in tensile strength and Young's modulus for the materials with various amounts of vitamin B_2 compared to the neat TPS film. This behavior indicates the presence of more hydrophilic groups in the samples as a function of higher content of VB. According to the literature [39,40], more absorbed humidity can act as an additional plasticizer. Herein, the lower tensile strength of the vitamin-reinforced TPS (TPS-VB1, TPS-VB5, and TPS-VB10) films with the higher vitamin B_2 content can be attributed to the existence of more pores in the TPS matrix. However, it was observed that the incorporation of BC into the TPS/VB film led to a substantial increase in tensile strength and Young's modulus. The explanation of this phenomenon may consist of two performances of silicate layers, including the reinforcing effect of clay particles and blocking of the pores created by the addition of vitamin B_2. The most important role of vitamin concentration was demonstrated in the mechanical properties by the values of tensile strength for 5 php VB. This increase may have been facilitated by interactions among starch chain, clay particles and VB, in which many factors, including the ratio of amylose-amylopectin in starch, dispersion and exfoliation of BC, and the amount of VB can play a critical role [9]. It is well-known that plasticizers are also essential additives since they can improve the flexibility and handling of films, maintain integrity, and avoid pores and cracks in the polymeric matrix [41,42]. From this point of view, the action of VB as a plasticizer for starch molecules should be considered as

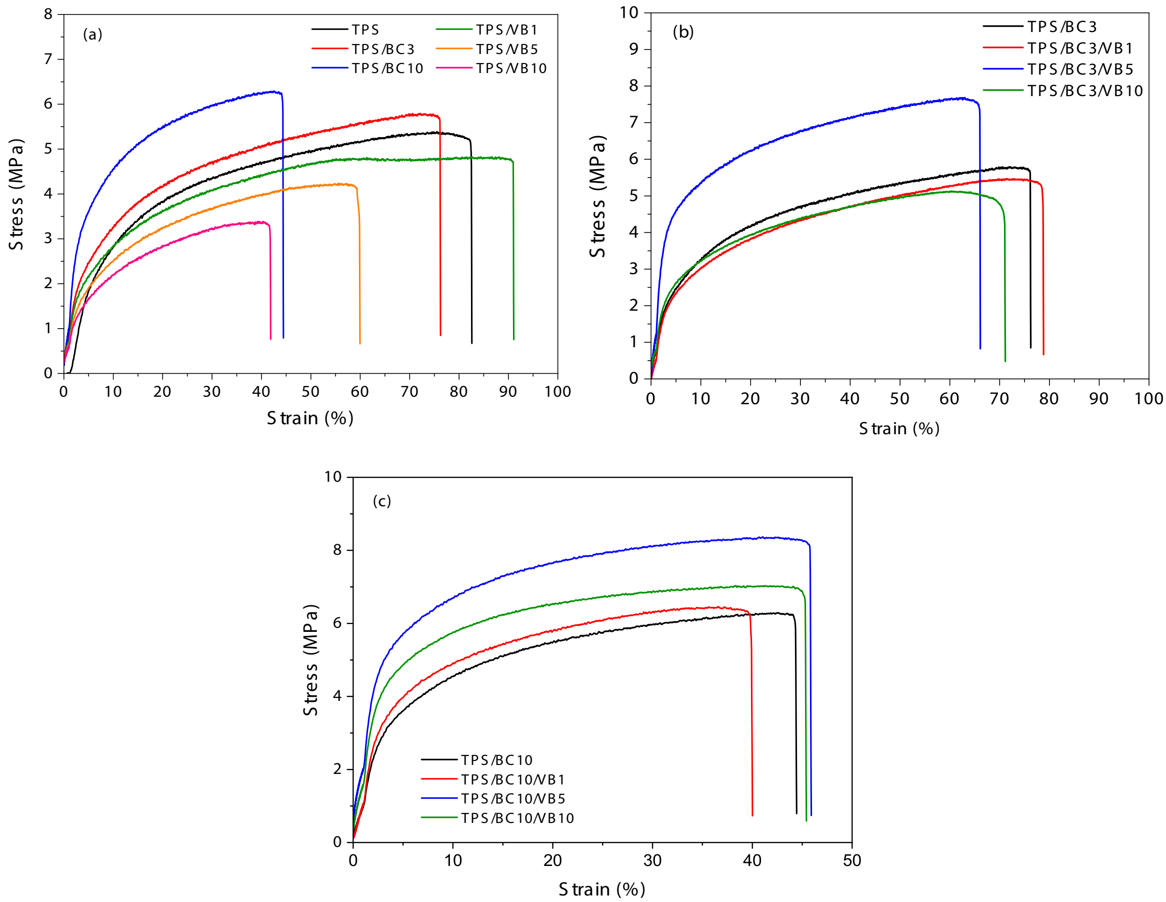

Fig. 5. Stress–strain curves for (a) thermoplastic starch (TPS)/bentonite clay (BC) nanocomposite and TPS/vitamin B_2, (b) TPS/BC3 with various contents of vitamin B_2, and (c) TPS/BC10 with various contents of vitamin B_2. The concentration is shown in php as the number after each code.

another factor to explain this result. Consequently, use of an optimum amount of VB and BC can cause synergistic effects on mechanical properties. This explanation is supported by the shape of the stress–-strain curves for the TPS nanocomposites displayed in Fig. 5.

3.4. Dynamic mechanical thermal analysis (DMTA)

The mechanical response of the sample under a small harmonic force was recorded in DMTA measurements. Also, the viscoelastic response of polymers, which is associated with the molecular motions related to internal changes of the polymers, was evaluated by this technique. Relaxation processes undergoing in the studied samples during gradual heating can be detected through inflection points in storage modulus as well as maxima in both the loss modulus and the damping factor temperature dependences as some deal of received energy dissipates through viscous movement [43]. The storage modulus obtained from the DMTA analysis of the TPS nanocomposite films are shown in Fig. 6. The storage modulus (G′) of samples containing BC and VB was higher than the neat TPS film. It has been known that the storage modulus was associated with stiffness, which was affected by the glass transition temperature (T_g), morphology, and structure of the polymer matrix. This observation may be related to the interactions among starch chain, clay particles, and VB, which was indicated by the mechanical properties (Fig. 4).

Fig. 7 represents the tan δ curves as a function of temperature. Tan δ is the viscoelasticity index of the material, which is usually defined as a damping term. The temperatures of the appearance of maximum tan δ determined from data in Fig. 7, are displayed in Table 4. Theoretically, in tan δ temperature dependences of TPS with higher plasticizer contents, two relaxation peaks usually appear which reflected the partial miscibility of starch and glycerol. The first one close to the glass transition temperature of the plasticizer is related to the glycerol-rich domains, in which the mobility of starch chains is controlled by glycerol molecules motion. The second relaxation temperature corresponds to the starch-rich domains [40,44]. As seen in Table 4, the main relaxation of the starch-rich phase shifted to the higher temperatures with rising vitamin B_2 content for TPS/BC/VB nanocomposites. This observation can be explained by the interaction among the starch, glycerol, BC, and VB, thus restricting the mobility of the starch chains. Therefore, the macromolecules are restricted in motion so that their segmental relaxation is observed at higher temperatures [45,46]. Table 4 shows that the relaxation temperature for TPS/VB samples increased, reaching a maximum for TPS/VB5 sample, then slightly decreased for TPS/VB10. This trend can be attributed to the existence of high amounts of hydrophilic groups in the TPS/VB10 sample. Interestingly, in the case of TPS nanocomposite containing 5 php of VB, a broad relaxation peak was observed with a higher intensity compared to the other samples, indicating strong interaction among the components. These results were also supported by a substantial increase in both tensile strength and Young's modulus.

3.5. Thermogravimetric analysis (TGA)

Thermal stability and degradation profile of the prepared samples were evaluated by TGA. Fig. 8 shows the thermal behavior of bentonite-reinforced nanocomposites containing vitamin B_2. The initial weight loss observed in the temperature range of 20–200 °C is attributed to the elimination of unbonded and bonded water molecules [47]. Two distinct stages of mass loss from 220 to 350 °C correspond to the degradation of starch and vitamin B_2, verifying the compatibility of vitamin with

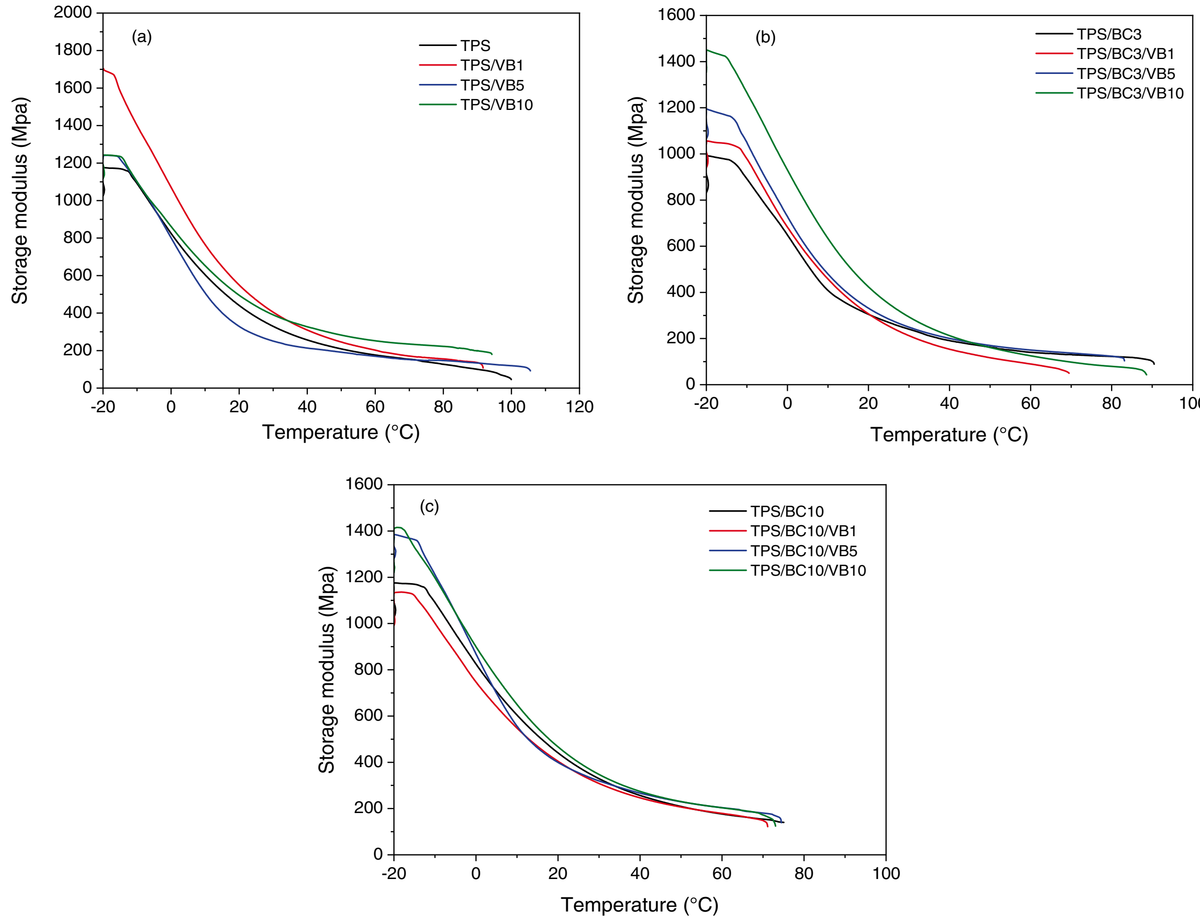

Fig. 6. Temperature dependences of the storage modulus for the (a) TPS/VB, (b) TPS/bentonite clay (BC) 3 with various contents of vitamin B_2 (VB), and (c) TPS/BC10 with various contents of VB. The concentration is shown in php as the number after each code.

starch. Starch was found to degrade between 300 and 500 °C [48]. It was reported that vitamin B_2 firstly decomposed at ribo block by losing three molecules of water resulting in the formation of alcohol, ethylene, and acetaldehyde. The second weight loss for vitamin B_2 at a temperature over 250 °C is attributed to the degradation of flavin block which leads to the formation of CO_2, phenol, and char [49,50].

The temperatures corresponding to the weight losses of 10 %, 50 %, 70 %, and 90 % are presented in Table 5. The onset of decomposition for TPS/BC3/VB5, TPS/BC3/VB10, TPS/BC10/VB1, TPS/BC10/VB5, and TPS/BC10/VB10 is occurred at around 230, 232, 245, 234, and 238 °C, respectively. As proved in thermal patterns, increase of the amount of bentonite from 3 php to 10 php resulted in increase of the thermal stability of nanocomposites. These findings are in agreement with the previous reports on improving the thermal resistance of nanocomposites in the presence of bentonite [51,52] or MMT [53,54]. Clay-reinforced nanocomposites were found to form char with a multilayered carbonaceous silicate structure during pyrolysis. This leads to preserving its structure in the polymer matrix at temperatures over 500 °C. The carbonaceous-silicate char formed on the film's surface acts as an insulator and delays the release of components produced during decomposition [55]. As revealed in Fig. 8, inorganic residue increased for the nanocomposites containing 10 php BC compared to those containing 3 php BC. This increment at around 800 °C further approves the successful incorporation of BC into the starch matrix.

3.6. Water uptake behaviors and weight loss

The effect of BC and VB was studied on the water uptake of TPS and the results are presented in Fig. 9. As shown, the water uptake ratio of TPS film decreased by incorporating 3 php of BC. This finding may be ascribed to the interaction between BC and the polymer, which prevents water diffusion into the nanocomposite. In contrast, the water uptake ratio of TPS film increased with the addition of 10 php BC (TPS/BC10). It was reported that the interaction between starch and BC increased the surface hydrophilicity facilitating the diffusion of water molecules [56]. This behavior may be concluded from the increased porosity of the composites. Moreover, the high specific surface area of the nanoplatelets of bentonite, provides the perfect contact with starch which leads to a reduction in the permeability of the composites [57].

The water uptake ratio for TPS films reinforced with 1 php and 5 php of vitamin B_2 showed an increase compared to TPS film. This result can be attributed to the higher affinity of vitamin B_2 to absorb water, which enhances the hydrophilicity of vitamin-reinforced TPS composite. This finding is consistent with the published data on the increase of the swelling degree of riboflavin-loaded chitosan [58]. Whereas, further increase of vitamin B_2 (10 php) caused a decrease in the water uptake ratio. The reason for the decrease may consist in the effective reactions between functional groups of starch and vitamin, which formed a more compact structure, limiting the penetration of water molecules into the matrix [59].

Since solubility is determined as the main criterion for measuring the water resistance of the prepared films, the degradation behavior of TPS-based nanocomposites was studied by measuring their solubility after regular incubation times (10, 24, and 48 h) in PBS (pH 7.4) at 37 °C. As shown in Fig. 10, the weight loss for all of the prepared samples increased with increasing incubation time. It was also revealed that the addition of both BC and VB in TPS films influenced the degradation rate of the nanocomposite. The incorporation of BC into TPS film

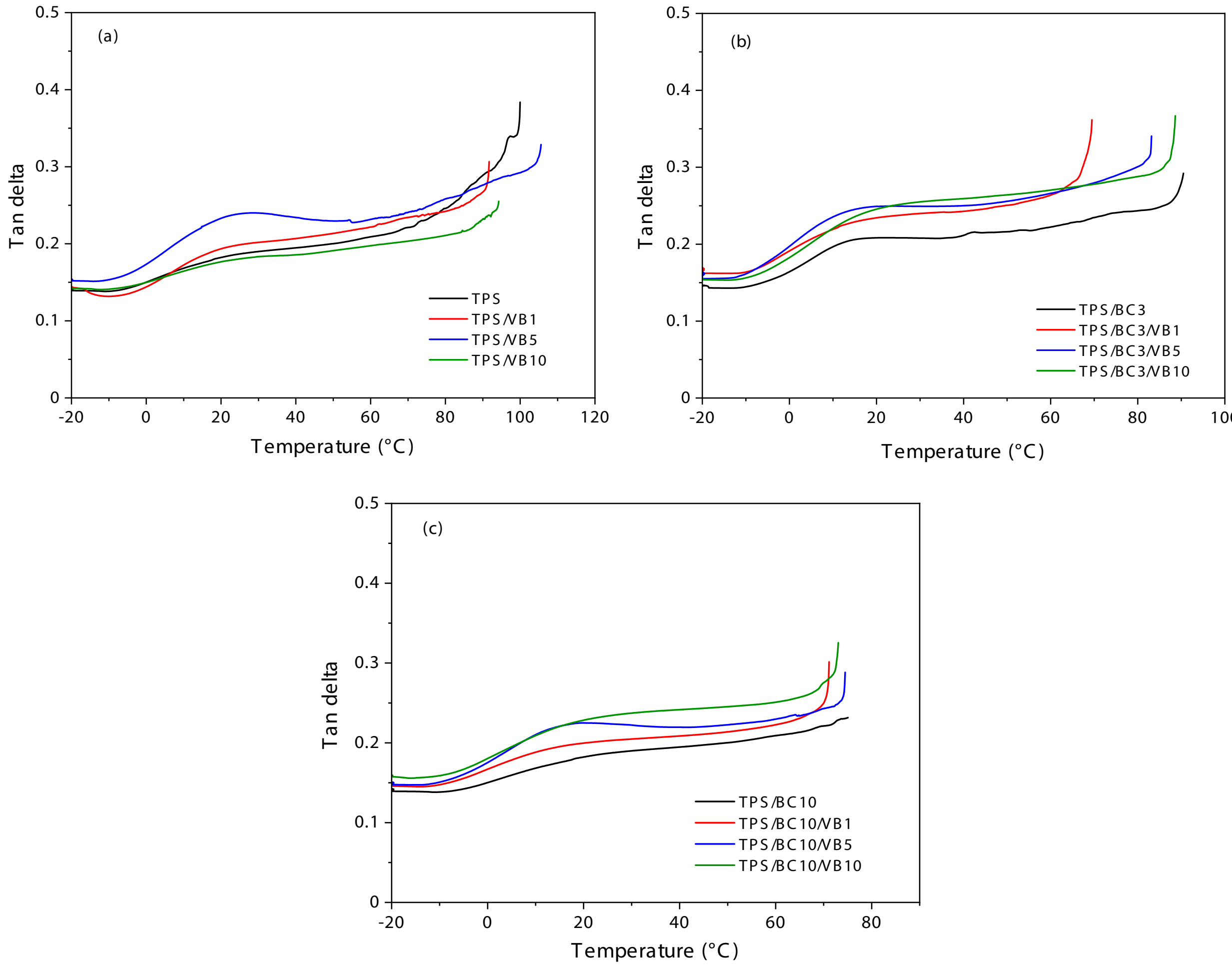

Fig. 7. Temperature dependences of the tan δ for the (a) TPS/VB, (b) TPS/bentonite clay (BC) 3 with various contents of vitamin B_2 (VB), and (c) TPS/BC10 with various contents of VB. The concentration is shown in php as the number after each code.

Table 4
Temperatures of the appearance of maximum tan δ determined from data in Fig. 6b.

Sample code	Peak T (°C)
TPS	19.3
TPS/VB1	19.2
TPS/VB5	24.6
TPS/VB10	23.2
TPS/BC3	13.6
TPS/BC3/VB1	13.6
TPS/BC3/VB5	14.2
TPS/BC3/VB10	16.9
TPS/BC10	19.3
TPS/BC10/VB1	14.0
TPS/BC10/VB5	15.3
TPS/BC10/VB10	17.0

significantly decreased the solubility of the nanocomposite, which could hinder the water penetration into the matrix. This result may occur due to the formation of strong hydrogen bonds between hydroxyl groups of BC and the hydroxyl groups of starch, which may increase the cohesiveness of the nanocomposite matrix and decrease their water sensitivity [60].

3.7. Zeta potential of TPS films

The zeta potential of TPS surfaces with different compositions was investigated in this study, and the results are presented in Fig. 11. All TPS films exhibited negative charge values, and the charge of TPS alone was found to be close to zero. The negative charge observed in TPS films containing VB can be attributed to the presence of VB with negative charge [25]. The net charge of the films decreased with the addition of BC, which could be explained by the incorporation of VB and BC, both

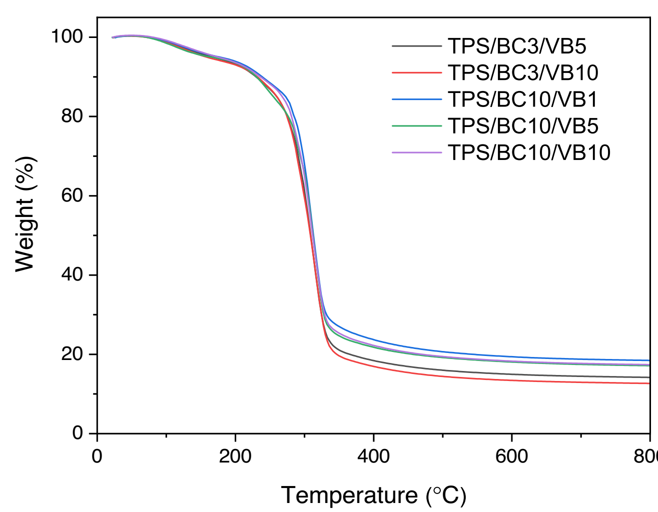

Fig. 8. TGA thermograms of TPS composite samples filled with various contents of bentonite clay (BC) and vitamin B_2 (VB).

Table 5
Temperatures corresponded to weight losses of 10 %, 50 %, 70 %, and 90 %.

Sample	T (°C)			
	10 %	50 %	70 %	90 %
TPS/BC3/VB5	230.3	307.1	324.3	917.5
TPS/BC3/VB10	233.0	307.1	324.4	912.2
TPS/BC10/VB1	245.0	313.0	332.0	956.0
TPS/BC10/VB5	232.8	312.3	326.0	943.4
TPS/BC10/VB10	238.3	312.4	329.5	948.4

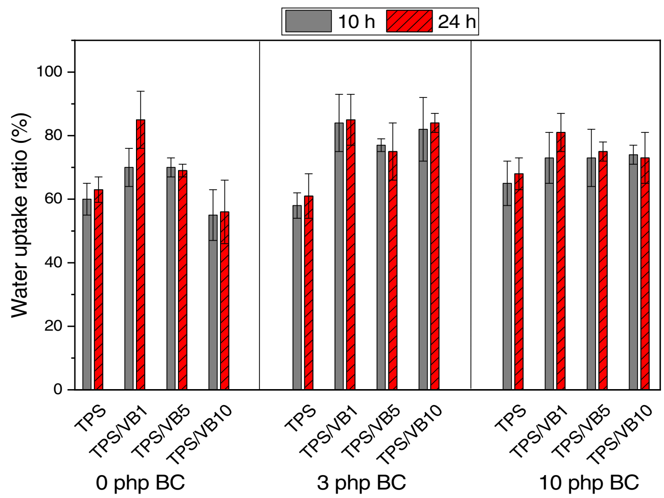

Fig. 9. Water uptake of TPS nanocomposite films filled with various contents of bentonite clay (BC) and vitamin B_2 (VB) in water measured during 24 h. The concentration is shown in php as the number after each code.

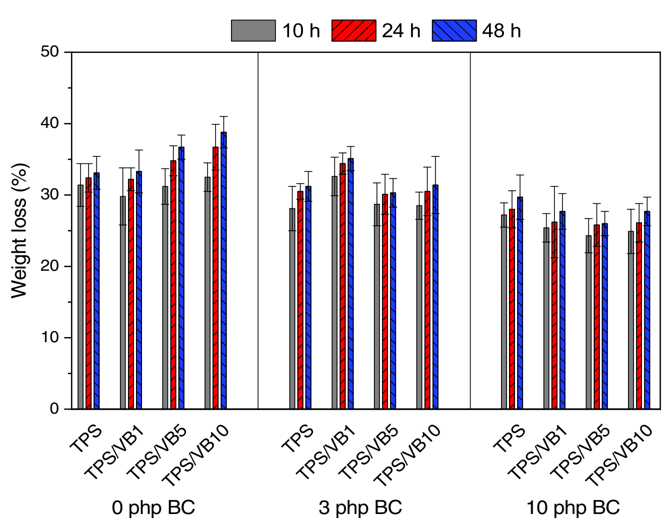

Fig. 10. Weight loss (in %) of the TPS nanocomposite filled with various contents of bentonite clay (BC) and vitamin B_2 (VB) in water for 48 h. The concentration of VB is shown in php as the number after each code.

having a negative charge, into TPS samples. These findings suggest that the incorporation of BC and VB into TPS films affects the surface charge of the resulting films.

3.8. *Release behavior of vitamin B_2 from nanocomposite*

The release profiles of VB from the prepared nanocomposites during 96 h are presented in Fig. 12. At a glance, Fig. 12 shows that the release

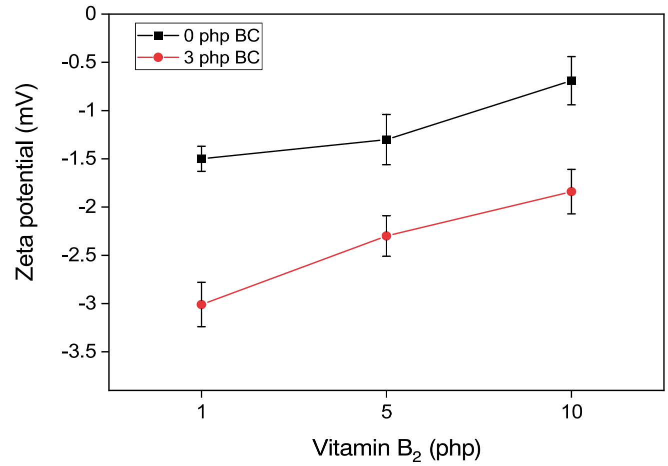

Fig. 11. Zeta potential (mV) of TPS samples with varying content of bentonite clay and vitamin B_2.

of VB from nanocomposites depends on the content of BC, the higher BC content, the slower VB release. The released VB from TPS/VB1 was 52 %, which decreased to 42 % and 27 % in the presence of 3 and 10 php BC, respectively. On the other hand, around 80 % of VB was released from TPS/VB5, while the release content reached 64 % and 52 % after incorporating 3 and 10 php BC, respectively. The incorporation of 3 and 10 php of BC into TPS/VB10 resulted in decrease of the vitamin release from 60 % to 50 % and 46 %, respectively. It is also clear that more sustained VB release was attained in BC-reinforced TPS/VB. This behavior might be ascribed to the barrier properties of the clay, which hinders the fast penetration of hydrophilic VB into aqueous media by creating a tortious path, as described by the effect of clay on the release of VB and various drugs in the literature [61–64].

4. Conclusions

The present study provides important insights into the development of TPS/BC nanocomposite reinforced with VB, which has potential applications in various fields, including packaging, food, and pharmaceuticals. The results revealed that the incorporation of VB and BC into TPS matrix could substantially enhance the mechanical properties of the composite. The synergistic effect of VB and BC was observed at a specific concentration of 5 php VB and 3 php BC, which exhibited the highest increase in tensile strength and Young's modulus. Moreover, the nanocomposites demonstrated an increase in the main relaxation of the starch-rich phase with the rising VB content, which indicates the restriction of the mobility of the starch chains. These results indicate that TPS/BC/VB composites have excellent mechanical properties that can be tailored by adjusting the VB and BC concentrations.

Additionally, the TPS/BC/VB composites demonstrated good potential for vitamin delivery purposes. The release studies indicate that the TPS nanocomposites with a higher BC content resulted in a lower amount and delayed vitamin release, indicating that the release of VB can be controlled by adjusting the BC content. Furthermore, the TPS nanocomposites reinforced with VB showed an increase in water uptake, which could be beneficial for certain applications, such as in the food industry. Overall, the results suggest that TPS/BC/VB composites have potential as biodegradable and renewable materials for various applications and pave the way for further research in this area.

CRediT authorship contribution statement

Abolfazl Heydari: Conceptualization, Methodology, Supervision, Funding acquisition, Writing - Reviewing and Editing. **Milad Khaje-Hassani:** Investigation, Methodology, Writing - Original Draft. **Haniyeh**

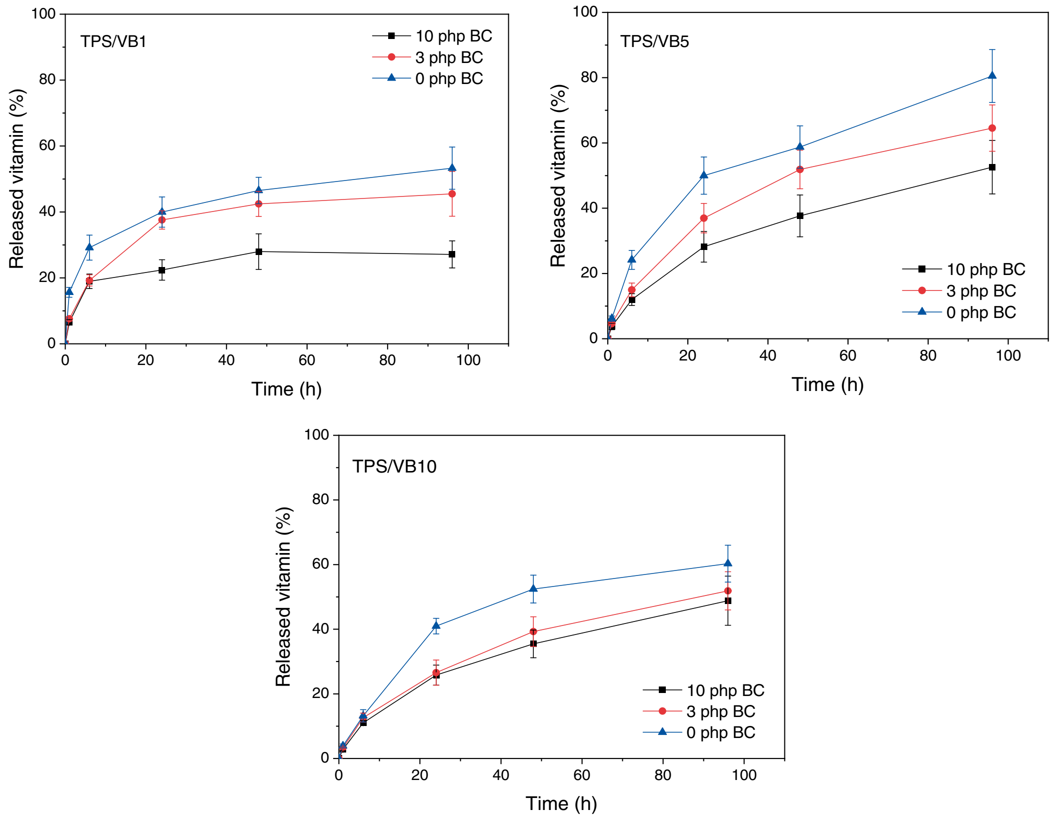

Fig. 12. Cumulative release of VB from thermoplastic starch/bentonite clay nanocomposite in PBS (pH 7.4). Each graph shows the release of vitamins (in %) from TPS nanocomposite containing various contents of BC in php and the same content of VB. The concentration of VB is shown in php as the number after each code.

Daneshafruz:** Investigation, Methodology, Writing - Original Draft. **Sepideh Hamedi:** Formal analysis, Writing - Reviewing and Editing. **Faeze Dorchei:** Investigation, Methodology, Writing - Reviewing and Editing. **Mário Kotlár:** Investigation, Methodology. **Fahimeh Kazeminava:** Formal analysis, Methodology, Writing - Reviewing and Editing. **Samahe Sadjadi:** Formal analysis, Writing - Reviewing and Editing. **Farideh Doostan:** Supervision, Funding acquisition, **Ivan Chodak:** Supervision, Writing - Reviewing and Editing. **Hassan Sheibani:** Supervision, Writing - Reviewing and Editing.

Declaration of competing interest

The authors declare that they have no known competing financial interests or personal relationships that could have appeared to influence the work reported in this paper.

Acknowledgment

The authors express their gratitude to the Endocrinology and Metabolism Research Center of Kerman University of Medical Sciences and Shahid Bahonar University of Kerman. This work was also supported by the Slovak Research and Development Agency under the contract number APVV-18-0480 and VEGA Grant Agency under contract number 2/0121/23. This work is the result of the project implementation Advanced bioactive hydrogel scaffolds for regenerative medicine (ABSACARM), ITMS2014+: 313011BWL6 supported by the Operational Programme Integrated Infrastructure funded by the European Regional Development Fund.

References

[1] H. Peidayesh, A. Heydari, K. Mosnackova, I. Chodak, In situ dual crosslinking strategy to improve the physico-chemical properties of thermoplastic starch, Carbohydr. Polym. 269 (2021), 118250.
[2] H. Peidayesh, Z. Ahmadi, H.A. Khonakdar, M. Abdouss, I. Chodak, Baked hydrogel from corn starch and chitosan blends cross-linked by citric acid: preparation and properties, Polym. Adv. Technol. 31 (6) (2020) 1256–1269.
[3] F. Ivanic, D. Jochec-Moskova, I. Janigova, I. Chodak, Physical properties of starch plasticized by a mixture of plasticizers, Eur. Polym. J. 93 (2017) 843–849.
[4] S.M. Amaraweera, C. Gunathilake, O.H.P. Gunawardene, N.M.L. Fernando, D. B. Wanninayaka, R.S. Dassanayake, S.M. Rajapaksha, A. Manamperi, C.A. N. Fernando, A.K. Kulatunga, A. Manipura, Development of starch-based materials using current modification techniques and their applications: a review, Molecules 26 (22) (2021) 6880.
[5] M. Xiaofei, Y. Jiugao, F. Jin, Urea and formamide as a mixed plasticizer for thermoplastic starch, Polym. Int. 53 (11) (2004) 1780–1785.
[6] T.Y. Ke, X.Z. Sun, Physical properties of poly(lactic acid) and starch composites with various blending ratios, Cereal Chem. 77 (6) (2000) 761–768.
[7] H. Peidayesh, K. Mosnackova, Z. Spitalsky, A. Heydari, A.O. Siskova, I. Chodak, Thermoplastic starch-based composite reinforced by conductive filler networks: physical properties and electrical conductivity changes during cyclic deformation, Polymers 13 (21) (2021) 3819.
[8] S. Pavlidou, C.D. Papaspyrides, A review on polymer-layered silicate nanocomposites, Prog. Polym. Sci. 33 (12) (2008) 1119–1198.
[9] V.P. Cyras, L.B. Manfredi, M.T. Ton-That, A. Vazquez, Physical and mechanical properties of thermoplastic starch/montmorillonite nanocomposite films, Carbohydr. Polym. 73 (1) (2008) 55–63.
[10] A. Heydari, H. Sheibani, Fabrication of poly(β-cyclodextrin-co-citric acid)/bentonite clay nanocomposite hydrogel: thermal and absorption properties, RSC Adv. 5 (100) (2015) 82438–82449.
[11] A. Heydari, H. Khoshnood, H. Sheibani, F. Doostan, Polymerization of β-cyclodextrin in the presence of bentonite clay to produce polymer nanocomposites for removal of heavy metals from drinking water, Polym. Adv. Technol. 28 (4) (2017) 524–532.
[12] D. Borah, H. Nath, H. Saikia, Modification of bentonite clay & its applications: a review, Rev. Inorg. Chem. 42 (3) (2022) 265–282.
[13] G. Santagata, F. Valerio, A. Cimmino, G. Dal Poggetto, M. Masi, M. Di Biase, M. Malinconico, P. Lavermicocca, A. Evidente, Chemico-physical and antifungal properties of poly(butylene succinate)/cavoxin blend: study of a novel bioactive polymeric based system, Eur. Polym. J. 94 (2017) 230–247.

[14] I. Katouzian, S.M. Jafari, Nano-encapsulation as a promising approach for targeted delivery and controlled release of vitamins, Trends Food Sci. Technol. 53 (2016) 34–48.
[15] A. Orsuwan, S. Kwon, N. Bumbudsanpharoke, S. Ko, Novel LDPE-riboflavin composite film with dual function of broad-spectrum light barrier and antimicrobial activity, Food Control 100 (2019) 176–182.
[16] H.J. Powers, Riboflavin (vitamin B-2) and health, Am. J. Clin. Nutr. 77 (6) (2003) 1352–1360.
[17] A. Djoullah, R. Saurel, Controlled release of riboflavin encapsulated in pea protein microparticles prepared by emulsion-enzymatic gelation process, J. Food Eng. 292 (2021), 110276.
[18] J. Pei, S. Zhu, Y. Liu, Y. Song, F. Xue, X. Xiong, C. Li, Photodynamic effect of riboflavin on chitosan coatings and the application in pork preservation, Molecules 27 (4) (2022) 1355.
[19] R. Casadey, C. Challier, M. Altamirano, M.B. Spesia, S. Criado, Antioxidant and antimicrobial properties of tyrosol and derivative-compounds in the presence of vitamin B2. Assays of synergistic antioxidant effect with commercial food additives, Food Chem 335 (2021) 127576.
[20] N. Suwannasom, I. Kao, A. Pruss, R. Georgieva, H. Baumler, Riboflavin: the health benefits of a forgotten natural vitamin, Int. J. Mol. Sci. 21 (3) (2020) 950.
[21] K. Thakur, S.K. Tomar, B. Brahma, S. De, Screening of riboflavin-producing lactobacilli by a polymerase-chain-reaction-based approach and microbiological assay, J. Agric. Food Chem. 64 (9) (2016) 1950–1956.
[22] A. Yepez, P. Russo, G. Spano, I. Khomenko, F. Biasioli, V. Capozzi, R. Aznar, In situ riboflavin fortification of different kefir-like cereal-based beverages using selected andean LAB strains, Food Microbiol. 77 (2019) 61–68.
[23] F.Nur Parin, Retrospective, Perspective and Prospective of B-Complex Vitamins: Encapsulation of Vitamins and Release From Vitamin-loaded Polymers, B-Complex Vitamins - Sources, Intakes and Novel Applications, 2022.
[24] A. Heydari, F. Mehrabi, T. Shamspur, H. Sheibani, A. Mostafavi, Encapsulation and controlled release of vitamin B2 using peracetyl-β-cyclodextrin polymer-based electrospun nanofiber scaffold, Pharm. Chem. J. 52 (1) (2018) 19–25.
[25] A. Heydari, F. Doostan, H. Khoshnood, H. Sheibani, Water-soluble cationic poly (β-cyclodextrin-co-guanidine) as a controlled vitamin B2 delivery carrier, RSC Adv. 6 (40) (2016) 33267–33278.
[26] H.J. Lee, G.M. Fernandes-Cunha, D. Myung, In situ-forming hyaluronic acid hydrogel through visible light-induced thiol-ene reaction, React. Funct. Polym. 131 (2018) 29–35.
[27] Y.C. Danarto, Rochmadi, budhijanto, microencapsulation of riboflavin (vitamin B2) using alginate and chitosan: effect of alginate and chitosan concentration upon encapsulation efficiency, IOP Conf. Ser. Mater. Sci. Eng. 858 (1) (2020), 012030.
[28] P. Mokhtari, M. Ghaedi, Water compatible molecularly imprinted polymer for controlled release of riboflavin as drug delivery system, Eur. Polym. J. 118 (2019) 614–618.
[29] S.K. Bajpai, S. Sharma, Dynamic release of riboflavin from ethyl cellulose coated barium alginate beads for gastrointestinal drug delivery: an in vitro study, J. Macromol. Sci. Pure A42 (5) (2005) 649–661.
[30] S.K. Bajpai, S. Saxena, Dynamic release of riboflavin from a starch-based semi IPN via partial enzymatic degradation: part II, React. Funct. Polym. 61 (1) (2004) 115–129.
[31] Z. Lv, Y.T. Hu, J.P. Guan, R.C. Tang, G.Q. Chen, Preparation of a flame retardant, antibacterial, and colored silk fabric with chitosan and vitamin B2 sodium phosphate by electrostatic layer by layer assembly, Mater. Lett. 241 (2019) 136–139.
[32] P. Liao, S. Dai, Z. Lian, X. Tong, S. Yang, Y. Chen, W. Qi, X. Peng, H. Wang, L. Jiang, The layered encapsulation of vitamin B2 and beta-carotene in multilayer alginate/chitosan gel microspheres: improving the bioaccessibility of vitamin B2 and beta-carotene, Foods 11 (1) (2021) 20.
[33] I.C. Carlan, B.N. Estevinho, F. Rocha, Innovation and improvement in food fortification: microencapsulation of vitamin B2 and B3 by a spray-drying method and evaluation of the simulated release profiles, J. Dispers. Sci. Technol. (2021) 1–13.
[34] K. Dean, L. Yu, D.Y. Wu, Preparation and characterization of melt-extruded thermoplastic starch/clay nanocomposites, Compos. Sci. Technol. 67 (3–4) (2007) 413–421.
[35] K. Majdzadeh-Ardakani, A.H. Navarchian, F. Sadeghi, Optimization of mechanical properties of thermoplastic starch/clay nanocomposites, Carbohydr. Polym. 79 (3) (2010) 547–554.
[36] P. Kampeerapappun, D. Aht-Ong, D. Pentrakoon, K. Srikulkit, Preparation of cassava starch/montmorillonite composite film, Carbohydr. Polym. 67 (2) (2007) 155–163.
[37] M.K.S. Monteiro, V.R.L. de Oliveira, F.K.G. dos Santos, E.L.D. Neto, R.H.D. Leite, E. M.M. Aroucha, K.N.D. Silva, Synergistic effect of the sequential intercalation of three types of surfactants in the exfoliation degree of bentonite clay in films of cassava, J. Mol. Liq. 266 (2018) 770–780.
[38] H. Peidayesh, Z. Ahmadi, H.A. Khonakdar, M. Abdouss, I. Chodak, Fabrication and properties of thermoplastic starch/montmorillonite composite using dialdehyde starch as a crosslinker, Polym. Int. 69 (3) (2020) 317–327.
[39] M. Esmaeili, G. Pircheraghi, R. Bagheri, Optimizing the mechanical and physical properties of thermoplastic starch via tuning the molecular microstructure through co-plasticization by sorbitol and glycerol, Polym. Int. 66 (6) (2017) 809–819.
[40] H. Schmitt, A. Guidez, K. Prashantha, J. Soulestin, M.F. Lacrampe, P. Krawczak, Studies on the effect of storage time and plasticizers on the structural variations in thermoplastic starch, Carbohydr. Polym. 115 (2015) 364–372.
[41] M.G.A. Vieira, M.A. da Silva, L.O. dos Santos, M.M. Beppu, Natural-based plasticizers and biopolymer films: a review, Eur. Polym. J. 47 (3) (2011) 254–263.
[42] M.A. Garcia, M.N. Martino, N.E. Zaritzky, Lipid addition to improve barrier properties of edible starch-based films and coatings, J. Food Sci. 65 (6) (2000) 941–947.
[43] X.G. Zhang, L.S. Loo, Study of glass transition and reinforcement mechanism in Polymer/Layered silicate nanocomposites, Macromolecules 42 (14) (2009) 5196–5207.
[44] P.M. Forssell, J.M. Mikkila, G.K. Moates, R. Parker, Phase and glass transition behaviour of concentrated barley starch-glycerol-water mixtures, a model for thermoplastic starch, Carbohydr. Polym. 34 (4) (1997) 275–282.
[45] H.M. Park, X.C. Li, C.Z. Jin, C.Y. Park, W.J. Cho, C.S. Ha, Preparation and properties of biodegradable thermoplastic starch/clay hybrids, Macromol. Mater. Eng. 287 (8) (2002) 553–558.
[46] O. Fričová, M. Hutníková, H. Peidayesh, DMA study of thermoplastic starch/montmorillonite nanocomposites, in: AIP Conference Proceedings, AIP Publishing LLC, 2021, p. 050004.
[47] P. Yousefi, S. Hamedi, E.R. Garmaroody, M. Koosha, Antibacterial nanobiocomposite based on halloysite nanotubes and extracted xylan from bagasse pith, Int. J. Biol. Macromol. 160 (2020) 276–287.
[48] G.M. Glenn, G. Bingol, B.-S. Chiou, A.P. Klamczynski, Z. Pan, Sodium bentonite-based coatings containing starch for protecting structures in wildfire emergency situations, Fire Saf. J. 51 (2012) 85–92.
[49] M.A. Sheraz, S.H. Kazi, S. Ahmed, Z. Anwar, I. Ahmad, Photo, thermal and chemical degradation of riboflavin, Beilstein J. Org. Chem. 10 (2014) 1999–2012.
[50] N. Ahmad, M. Alam, M.A.N. Al-Otaibi, Thermal decomposition and kinetic studies of solid riboflavin using model-free methods, Prog. React. Kinet. Mech. 40 (1) (2015) 86–94.
[51] M. Koosha, S. Hamedi, Intelligent chitosan/PVA nanocomposite films containing black carrot anthocyanin and bentonite nanoclays with improved mechanical, thermal and antibacterial properties, Prog. Org. Coat. 127 (2019) 338–347.
[52] T. Jose, S.C. George, M.G. Maya, H.J. Maria, R. Wilson, S. Thomas, Effect of bentonite clay on the mechanical, thermal, and pervaporation performance of the poly(vinyl alcohol) nanocomposite membranes, Ind. Eng. Chem. Res. 53 (43) (2014) 16820–16831.
[53] Y.M. Wang, J.P. Gao, Y.Q. Ma, U.S. Agarwal, Study on mechanical properties, thermal stability and crystallization behavior of PET/MMT nanocomposites, Compos. Part B 37 (6) (2006) 399–407.
[54] Y. Hattab, N. Benharrats, Electrical and thermal properties of PANI-mmt nanocomposites in strongly acidic aqueous media, Sn Appl. Sci. 1 (7) (2019) 750.
[55] A. Nouri, M.T. Yaraki, M. Ghorbanpour, S. Agarwal, V.K. Gupta, Enhanced antibacterial effect of chitosan film using Montmorillonite/CuO nanocomposite, Int. J. Biol. Macromol. 109 (2018) 1219–1231.
[56] H. Dai, Y. Huang, H. Huang, Eco-friendly polyvinyl alcohol/carboxymethyl cellulose hydrogels reinforced with graphene oxide and bentonite for enhanced adsorption of methylene blue, Carbohydr. Polym. 185 (2018) 1–11.
[57] H. Zhang, Y. Shi, X. Xu, M. Zhang, L. Ma, Structure regulation of bentonite-alginate nanocomposites for controlled release of imidacloprid, ACS Omega 5 (17) (2020) 10068–10076.
[58] L. Su, J. Huang, H. Li, Y. Pan, B. Zhu, Y. Zhao, H. Liu, Chitosan-riboflavin composite film based on photodynamic inactivation technology for antibacterial food packaging, Int. J. Biol. Macromol. 172 (2021) 231–240.
[59] M. Taghizadeh, S. Aryan, M. Rouhi, M.R. Sobhiyeh, F. Askari, M. Gholipourmalekabadi, S. Sohrabvandi, M.Z. Khajavi, S.M. Davachi, A. Abbaspourrad, R. Mohammadi, A.M. Mortazavian, Photo-crosslinked gelatin-polyvinyl alcohol composite films: UV-riboflavin treatment for improving functional properties, J Food Process Pres 44 (7) (2020), e14550.
[60] N. Noshirvani, B. Ghanbarzadeh, H. Fasihi, H. Almasi, Starch-PVA nanocomposite film incorporated with cellulose nanocrystals and MMT: a comparative study, Int. J. Food Eng. 12 (1) (2016) 37–48.
[61] R. Swain, S. Nandi, R.N. Sahoo, S.S. Swain, S. Mohapatra, S. Mallick, Bentonite clay incorporated topical film formulation for delivery of trimetazidine: control of ocular pressure and in vitro-in vivo correlation, J. Drug Deliv. Sci. Technol. 67 (2022), 102956.
[62] H. Tabasi, F. Oroojalian, M. Darroudi, Green clay ceramics as potential nanovehicles for drug delivery applications, Ceram. Int. 47 (22) (2021) 31042–31053.
[63] H. Kaygusuz, M. Uysal, V. Adimcilar, F.B. Erim, Natural alginate biopolymer montmorillonite clay composites for vitamin B2 delivery, J. Bioact. Compat. Pol. 30 (1) (2015) 48–56.
[64] R. Garcia-Vazquez, E.P. Rebitski, L. Viejo, C. de los Rios, M. Darder, E.M. Garcia-Frutos, Clay-based hybrids for controlled release of 7-azaindole derivatives as neuroprotective drugs in the treatment of Alzheimer's disease, Appl Clay Sci 189 (2020) 105541.